Journal of Neuroendocrinology, 2006, Vol. 18, 413–425 doi:10.1111/j.1365-2826.2006.01431.x

PC1/3 and PC2 Gene Expression and Post-Translational Endoproteolytic Pro-Opiomelanocortin Processing is Regulated by Photoperiod in the Seasonal Siberian Hamster (*Phodopus sungorus*)

M. Helwig,*† R. M. H. Khorooshi,‡ A. Tups,† P. Barrett,* Z. A. Archer,* C. Exner,† J. Rozman,† L. J. Braulke,† J. G. Mercer* and M. Klingenspor†

*Molecular Endocrinology Group, Division of Obesity and Metabolic Health, Rowett Research Institute, Aberdeen Centre for Energy Regulation and Obesity (ACERO), Aberdeen, UK.

†Department of Animal Physiology, Biology Faculty, Philipps University Marburg, Marburg, Germany.

‡Medical Biotechnology Centre, University of Southern Denmark, Odense, Denmark.

Key words: seasonal body weight regulation, proteolytic processing, photoperiod, prohormone convertases, POMC.

Abstract

A remarkable feature of the seasonal adaptation displayed by the Siberian hamster (*Phodopus sungorus*) is the ability to decrease food intake and body weight (by up to 40%) in response to shortening photoperiod. The regulating neuroendocrine systems involved in this adaptation and their neuroanatomical and molecular bases are poorly understood. We investigated the effect of photoperiod on the expression of prohormone convertases 1 (PC1/3) and 2 (PC2) and the endoproteolytic processing of the neuropeptide precursor pro-opiomelanocortin (POMC) within key energy balance regulating centres of the hypothalamus. We compared mRNA levels and protein distribution of PC1/3, PC2, POMC, adrenocorticotrophic hormone (ACTH), α-melanocyte-stimulating hormone (MSH), β-endorphin and orexin-A in selected hypothalamic areas of long day (LD, 16 : 8 h light : dark), short day (SD, 8 : 16 h light : dark) and natural-day (ND, photoperiod depending on time of the year) acclimated Siberian hamsters. The gene expression of PC2 was significantly higher within the arcuate nucleus (ARC, $P < 0.01$) in SD and in ND (versus LD), and is reflected in the day length profile between October and April in the latter. PC1/3 gene expression in the ARC and lateral hypothalamus was higher in ND but not in SD compared to the respective LD controls. The immunoreactivity of PC1/3 cleaved neuropeptide ACTH in the ARC and PC1/3-colocalised orexin-A in the latyeral hypothalamus were not affected by photoperiod changes. However, increased levels of PC2 mRNA and protein were associated with higher abundance of the mature neuropeptides α-MSH and β-endorphin ($P < 0.01$) in SD. This study provides a possible explanation for previous paradoxical findings showing lower food intake in SD associated with decreased POMC mRNA levels. Our results suggest that a major part of neuroendocrine body weight control in seasonal adaptation may be effected by post-translational processing mediated by the prohormone convertases PC1/3 and PC2, in addition to regulation of gene expression of neuropeptide precursors.

Seasonal animals such as the Siberian hamster (*Phodopus sungorus*) exhibit remarkable physiological and metabolic adaptations in response to the seasonally changing environment. These adaptations include changes in coat insulation and colour, reproductive activity, food intake and body weight (1). The drive to reduce food intake in shortening winter photoperiod persists even if food is provided *ad lib* demonstrating the importance of this regulatory energy balance mechanism. A key neuronal centre that regulates these physiological responses is the hypothalamus, an area of the central nervous system (CNS) that integrates photoperiodic and peripheral inputs in a complex network of interacting orexigenic and anorexigenic neuropeptides (2, 3). The Siberian hamster processes information on changing photoperiod through the pineal hormone, melatonin, and about internal energy stores via peripherally released hormones such

Correspondence to: Michael Helwig, Animal Physiology, Department of Biology, Philipps-University, Karl-von-Frisch-Str. 8, 35032 Marburg, Germany (e-mail: helwigmi@staff.uni-marburg.de).

as leptin and ghrelin, to generate appropriate responses in terms of energy balance regulation (4–6). The voluntary decrease in food intake and body weight in short day (SD) presumably reflects the increased activity of anorexigenic components of this neuroendocrine system. One of the neuropeptides that would meet this criterion is alpha-melanocyte-stimulating hormone (α-MSH) (7, 8), a product of the 30–32 kDa molecule pro-opiomelanocortin (POMC), which exerts an inhibitory control on food intake and energy storage through its action in the CNS at the melanocortin 3 and 4 receptors (9). Unexpectedly, previous studies demonstrated decreased gene expression of the precursor POMC in SD which could in principal result in lower concentrations of α-MSH during winter (10–12). However, most neuropeptide precursors such as POMC have to undergo post-translational processing by proteolytic cleavage before their products acquire biological activity. The post-translational process is accomplished by highly specific cleavage enzymes (prohormone convertases) and is therefore an essential step not only as a part of the protein biosynthetic process, but also as a regulatory step in neuropeptide synthesis. In mammals, prohormone convertases 1/3 (PC1/3) and 2 (PC2), which are members of the subtilisin-like proprotein convertases, have been identified to be responsible for the proteolytic processing of neuropeptides and peptide hormones in neuronal endocrine tissue (13).

Both PC1/3 and PC2 are expressed in neuroendocrine tissues such as hypothalamic neurones and cleave prohormones at paired basic residues. The biosynthesis of several major orexigenic and anorexigenic peptides derived from precursors within this neuroendocrine network is reliant on the post-translational activity of these enzymes. Neuropeptides such as neuropeptide-Y (NPY) (14), and cocaine- and amphetamine-regulated transcript (CART) (15), which are involved in the regulation of energy homeostasis and feeding, are subject to enzymatic processing by PC1/3 and PC2. Consequently, this system must be considered an extensive control mechanism in neuropeptide maturation. Interestingly, PC2 has been shown to be mainly involved in the production of the anorexigenic peptides, α-MSH and CART, whereas PC1/3 is responsible for the generation of potent orexigenic NPY in the hypothalamus (16–18).

The cleavage-specificity of PC1/3 and PC2 in POMC processing was reported by cell transfection experiments. It has been demonstrated that PC1/3 cleaves POMC into large intermediate molecules, such as adrenocorticotrophic hormone (ACTH) and β-lipotrophin, whereas PC2 subsequently cleaves ACTH and β-lipotrophin into α-MSH and β-endorphin, respectively (Fig. 1) (19, 20). Thus, coordinated cleavage activity of both prohormone convertases is necessary to process neuropeptide precursors such as POMC into specific neuropeptides. Because PC1/3 and PC2 are essential for the post-translational processing of various neuropeptide precursors, it is likely that changes in gene expression and biosynthesis have fundamental effects on the maturation of neuropeptides and hence energy homeostasis.

We hypothesised that POMC processing is photoperiodically regulated by differential expression of PC1/3 and PC2. It is likely that decreasing body weight in SD acclimated hamsters is associated with higher levels of anorexigenic neuropeptides

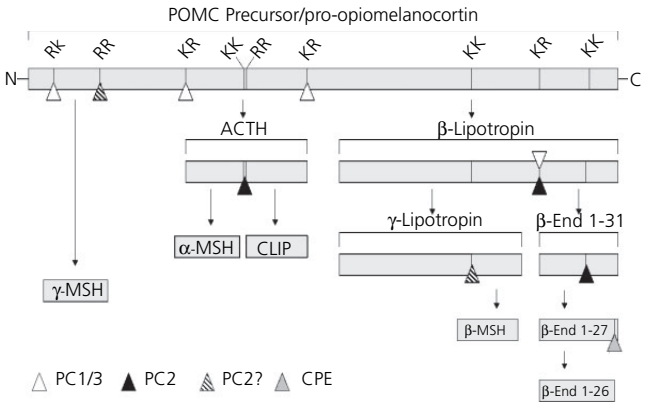

FIG. 1. Diagrammatic representation of post-translational endoproteolytic pro-opiomelanocortin (POMC) processing by prohormone convertases 1/3 (PC1/3) and 2 (PC2) and carboxypeptidase E (CPE). Cleavage sites are marked by paired basic amino acids R (Lysine) and K (Arginine). Sites believed but not confirmed as being processed by PC2 are indicated by hatched triangles. ACTH, Adrenocorticotrophic hormone; CLIP, corticotrophin-like intermediate peptide.

such as α-MSH despite down-regulated gene expression of POMC. We suggest that differential endoproteolytic activity of prohormone convertases in SD and long day (LD) is responsible for photoperiod-regulated biosynthesis of smaller POMC-derived neuropeptides. To test this, gene expression of PC1/3 and PC2 was investigated in hamsters exposed to ambient photoperiod in winter (October to April) to profile long-term effects. In addition, we measured mRNA expression levels of PC1/3 and PC2 following transfer of Siberian hamsters back into LD, after 14 weeks in artificial SD photoperiod. This experimental setup provided a better assessment of the temporal responsiveness of photoperiod-induced regulation of gene expression. Neuroanatomical protein distribution and differential expression of PC1/3, PC2, POMC, ACTH, α-MSH, and β-endorphin in SD and LD acclimated hamsters were investigated by immunohistochemistry. In a second approach, we used dual-fluorescence immunohistochemistry to colocalise the prohormone convertases with POMC and the derived neuropeptides to evaluate the ratio of proteolytic activity of PC1/3 and PC2 in SD and LD, respectively.

Previous reports have indicated neuroanatomical localisation of PC1/3 mRNA in the lateral hypothalamus (LH) (21), an important region of energy balance regulation (22) containing various potential targets for PC1/3 cleavage. As a consequence, we also focused on a neuropeptide precursor candidate for post-translational modification within this region. Although POMC is not expressed in this region, several pro-forms of different neuropeptides have been localised in the LH including pro-dynorphin (23), pro-melanin-concentrating hormone (24) and pro-orexin (25). All of these molecules are precursors of anabolic neuropeptides that exert opposing effects to those derived from POMC in the arcuate nucleus (ARC) (26). Pro-orexin was selected for investigation because we previously observed PC1/3 mRNA localised in prepro-orexin mRNA expressing neurones in the LH, which suggested a functional relationship of these neuroendocrine components. These recent observations at the mRNA level were extended to the protein level using immunohistochemical methods.

Materials and methods

Animals and experimental procedures

All described procedures were performed in accordance with German animal welfare regulation, or were licensed under the UK Home Office Animals (Scientific Procedures) Act, 1986, and had local ethical approval.

Siberian hamsters (*P. sungorus*) were drawn from breeding colonies established in the Biology Faculty in Marburg (Germany) and at the Rowett Research Institute in Aberdeen (Scotland). All animals were housed individually and had *ad lib* access to food (Marburg: Standard breeding chow diet, 7014, Altromin, Lage, Germany; Aberdeen: Labsure pelleted diet, Special Diet Services, Witham, UK) and water. Body weights were assessed weekly. Photoperiods referred to in this article are defined as LD (long day, 16 : 8 h light : dark), SD (short day, 8 : 16 h light : dark) and ND (natural day, with day length depending on time of the year).

Experiment 1

Siberian hamsters (n = 72, Marburg colony) were born and reared in ND at 23 °C. At the age of 4–6 months, they were divided into two groups. One group (n = 36, matched for sexes) was transferred to LD whereas the other (n = 36, matched for sexes) was maintained in ND and exposed to the progressive change in natural day length from October until April. At intervals of 40 days (October, November, January, February, March, April), hamsters from the LD and ND group (three males, three females per group) were killed with CO_2 and decapitated. Brains were immediately dissected, frozen on dry ice and stored at − 80 °C until required. The day length in ND photoperiod was calculated using the Sunrise/Sunset Calculator software (National Oceanic and Atmospheric Administration, Washington, DC, USA) based on the geographical location of the breeding facility in Marburg (8°46′17, 7′/50°48′17, 5′).

Experiment 2

Male Siberian hamsters (n = 32, Aberdeen colony) were housed individually at 22 °C. Hamsters used in this experiment were born and reared in LD. When they were 4–6 months old, half the animals (n = 16) were transferred to SD. After 14 weeks (week 0), a group of LD and SD hamsters (n = 4/group) were killed by cervical dislocation. All the remaining SD hamsters were transferred back to LD photoperiod. LD controls and hamsters transferred back from SD to LD (n = 4 per group) were then killed at intervals of 2 weeks (week 2, 4 and 6; 27). Brains were immediately dissected, frozen on dry ice and stored at −80 °C until required.

In situ *hybridisation*

Messenger RNA levels for PC1/3 and PC2 were quantified by *in situ* hybridisation in 15-μm coronal sections. Sections were collected throughout the extent of the hypothalamus onto two sets of 12 slides with six or seven sections mounted on each slide. Accordingly, slides spanned the lateral hypothalamic region approximating from −1.5 mm to −3.2 mm and the arcuate nucleus from −1.8 mm to −3.7 mm relative to Bregma, according to the atlas of the golden hamster brain (27). Two slides (one per set) from each animal were hybridised with a Siberian hamster specific PC1/3 or PC2 riboprobe cloned from cDNA, using techniques described in detail elsewhere (28). A control was performed by hybridising sections with equal length sense riboprobes of PC1/3 and PC2 resulting in no signal. Riboprobes complementary to partial fragments of PC1/3 and PC2 gene were generated from cloned Siberian hamster brain cDNA. The amplification of the PC1/3 (248 bp, GenBank AY625692) and PC2 (232 bp GenBank AY625693) fragments was performed by PCR using the primers: 5′-ATGGGGGTCGTCAAGGAG-ATAACT-3′ and 5′-GATGCCAGCAGCAGCCAGAGGTG-3′ (rat PC1/3, GenBank M76705) and 5′-GCGGCCGGGCTTCTCTTCT-3′ and 5′-GCT-GCCGCTTGTGATGTAGG-3′ (rat PC2, GenBank M76706), respectively. Both DNA fragments were ligated into pGEM-T-easy (Promega, Madison, WI, USA), transformed into *Escherichia coli* DH5α and sequenced. Sequence alignment of the species-specific fragments cloned from *P. sungorus* revealed a 96.4% (PC1/3) and 97% (PC2) identity to rat prohormone convertases at the nucleotide level. Sections were fixed, acetylated, and hybridised overnight at 58 °C using ^{35}S-labelled antisense riboprobes (1–1.5 × 10^7 d.p.m./ml). Slides were treated with RNase A to remove unhybridised probe and then desalted with a final high stringency wash in 0.1 × saline-sodium citrate (SSC) at 60 °C for 30 min. Hybridised slides were apposed with Kodak BioMax MR film (Kodak, Rochester, NY, USA) and, where appropriate, were coated with LM-1 film emulsion (Amersham, Bucks, UK). The levels of hypothalamic mRNAs were analysed and quantified by computerised densitometry (Image Pro-Plus software, Version 5.5.1; Media Cybernetics, Wokingham, Berkshire, UK) of *in situ* hybridisation autoradiograms. This determined the intensity and area of the hybridisation signal on the basis of set parameters; the integrated intensity was then computed using standard curves generated from ^{14}C autoradiographic microscales (Amersham). Image analysis was performed on representative sections, by an observer blind to the respective treatment groups, on four or five comparable sections spanning the ARC and three sections spanning the lateral hypothalamus. Micropictures of emulsion autoradiography sections were taken by bright field microscopy using an Olympus BX-50 microscope (Olympus Microscopes Ltd, Middlesex, UK) with attached digital camera system (Hitachi HV-C20, Hitachi Europe Ltd, Maidenhead, UK).

Dual immunostaining

Male Siberian Hamsters (n = 24, Aberdeen colony) were kept under conditions described above (Experiment 2). Half of them (n = 12) were transferred to SD. After 14 weeks in LD or SD, hamsters were anaesthetised with sodium pentobarbital and perfused with 4% paraformaldehyde (PFA) in 0.1 M phosphate-buffered saline (PBS, pH 7.4). Brains were dissected and transferred into a 4% PFA-PBS solution (8 h, 4 °C), followed by cryoprotection in 30% sucrose–0.1 M PBS (48 h, 4 °C), and were deep frozen in isopentane over dry ice (1 min). Coronal sections (35 μm) of the brain, corresponding to −1.5 to −3.7 mm relative to Bregma (27), were processed on a cryostat. Free-floating sections were treated with blocking solution (BS) containing 3% bovine serum albumin (BSA) in 0.5% Triton X-100–0.1 M PBS (0.5% PBS-T) for 1 h to block nonspecific reactions. Then, sections of LD (n = 3) and SD (n = 3) hamster brains were incubated with polyclonal rabbit anti-orexin-A (dilution 1 : 200, H-003–30, Phoenix Pharmaceuticals Inc., Belmont, CA, USA), anti-POMC (dilution 1 : 100, H-029–30, Phoenix), or anti-β-endorphin (dilution 1 : 100, H-022–33, Phoenix) in BS overnight (4 °C). Following washes in 0.25% PBS-T, sections were incubated for 2 h with unconjugated goat anti-rabbit Fab-fragment antibody (111-007-003, Jackson ImmunoResearch, West Grove, PA, USA) diluted 1 : 60 in BS at room temperature (RT). Sections were rinsed briefly in 0.25% PBS-T and incubated with Cy3 (Ex_{max} 554 nm, Em_{max} 566 nm) conjugated donkey anti-goat secondary antibody in BS (dilution 1 : 250, 705-165-147, Jackson) for 2 h at RT, rinsed again in 0.25% PBS-T and incubated with the second polyclonal rabbit anti-PC1/3 primary antibody (dilution 1 : 400, AB1260, Chemicon Inc., Temecula, CA, USA) or anti-PC2 (dilution 1 : 400, AB1262, Chemicon), in BS overnight at 4 °C. Sections were incubated with Alexa 488 dye (Ex_{max} 492 nm, Em_{max} 520 nm) conjugated goat anti-rabbit secondary antibody (dilution 1 : 250, Molecular Probes, Eugene, OR, USA) in BS for 2 h at RT. Colocalisation for α-MSH was performed with polyclonal sheep anti-α-MSH antibody (dilution 1 : 15.000, Chemicon) in BS overnight at 4 °C. In this case, different host species in which the applied primary antibodies were raised made an intermediate step of Fab-fragment incubation obsolete. α-MSH was visualised by incubation with Fluorescein (Ex_{max} 494 nm, Em_{max} 520 nm) conjugated donkey anti-sheep secondary antibody (dilution 1 : 100, AP184F, Chemicon) in BS for 2 h at RT. Incubation with the second primary antibodies and secondary antibody matched the steps described above. Sections were then rinsed in PBS, mounted on gelatin-coated slides, air-dried, dehydrated in graded alcohol, cleared in xylene and coverslipped with Enthelan (Merck Biosciences, Darmstadt, Germany). Sections were examined under a conventional Leica DMR epifluorescent microscope (Leica Microsystems, Wetzlar, Germany). Cell bodies were counted in two distinct hypothalamic regions, the lateral hypothalamus and the arcuate nucleus approximating from −1.5 mm to −3.2 mm (LH) and −1.8 mm to −3.7 mm (ARC) relative to Bregma, according to the atlas of the golden hamster brain (27). Immunoreactive (ir) cells in three (ARC) or four (LH) comparable sections of each individual animal were counted without knowledge of the experimental treatment. Total ir-cell number for each individual animal from the respective regions was calculated followed by the assessment of mean values for each experimental group. Images were taken by a digital camera system mounted on the microscope. Merging of images was performed by colour channel overlay using image processing software (Adobe Photoshop version 7.0; Adobe Systems Inc., San Jose, CA, USA). The anatomical localisation of neuropeptides within the brain of Siberian

hamsters was annotated according to the atlas of the golden hamster brain (27).

Controls

For controls, each of the primary antibodies was preincubated with its complementary peptide (α-MSH, 043-01, Phoenix; β-endorphin, 022-33, Phoenix; orexin-A, 003-30, Phoenix; POMC, 029-30, Phoenix; PC 1/3, AB5011, Abcam; PC2, AB5012, Abcam), prior to application. Incubation with preadsorbed primary antibodies resulted in no staining. Additional negative controls were performed by incubation of sections lacking primary antisera. Labelling of the primary antibodies by incubation with interchanged secondary antibodies showed an identical staining pattern.

Single immunostaining

Female Siberian hamsters (n = 20, Marburg colony) at 7 months of age were divided into two groups of 10. One group was kept in LD, whereas the other was transferred to SD. After 14 weeks, hamsters were killed in a CO_2 atmosphere and decapitated. Brains were excised, fixed in 4% PFA (48 h, 4 °C), and cryoprotected in 20% sucrose in 0.1 M PBS for 24 h at 4 °C. Brains were deep frozen in isopentane over dry ice (1 min) and stored in −80 °C until required. Coronal sections were cut on a cryostat at 30 μm. Endogenous peroxidase activity was inhibited in sections using 80% PBS, 10% methanol and 10% H_2O_2 for 15 min at RT. Free-floating sections were rinsed in PBS and 0.5% PBS-T. Following preincubation in a blocking solution containing 0.5% PBS-T and 3% BSA, sections were incubated with primary polyclonal rabbit anti-ACTH (Phoenix; H-001-21) antibody diluted 1 : 350 in BS overnight at 4 °C. Following washing in 0.5% PBS-T, sections were then incubated with peroxidase-conjugated goat anti-rabbit antibody (Jackson Immunoresearch, 111-035-144) diluted 1 : 500 in BS for 1 h at RT. Using Vector SG substrate kit for peroxidase (SK-4700, Vector Laboratories, Burlingame, CA, USA), the colour reaction resulted in dark-grey/blue immunostaining. Sections were then rinsed in PBS, mounted on gelatin-coated slides, air-dried, dehydrated in graded alcohol, cleared in xylene and coverslipped with Enthelan (Merck). Immunoreactive cell bodies were counted as for the dual-immunostaining protocol, using a Zeiss Axioskop (Carl Zeiss, Jena, Germany) microscope (objective, ×20). Images were taken by a mounted digital camera. Quantification and illustration of PC1/3, PC2, POMC, α-MSH, β-endorphin and orexin-A immunohistochemistry was performed on sections obtained from the dual-staining experiment described above. Micrographs showing the neuroanatomical distribution were colour inverted to greyscale mode using image editing software for enhanced visibility.

Controls

The specificity of primary antibody was tested by adding an excess of ACTH-(Phoenix; 001-21) peptide to the primary antibody for 3 h at RT before application to sections, or by omission of the primary antibody. Brain sections incubated either with preadsorbed primary antiserum or in the absence of primary antibodies did not exhibit any ACTH-ir (data not shown).

Statistical analysis

Data were analysed by two-way analysis of variance (ANOVA) followed by the Student–Newman–Keuls multiple comparison test, where appropriate (for *in situ* experiments), and one-way ANOVA (for immunohistochemistry data) using a statistical software package (SigmaStat, Jandel Corp, Richmond, VA, USA). Data from *in situ* hybridisation experiments are presented as means ± SEM; Data for immunohistochemistry experiments are presented as percentage values of LD control ± SEM. $P < 0.05$ was considered statistically significant.

Results

Effect of seasonal changing photoperiod on body weight

The body weight trajectory of ND animals was inversely related to the seasonal change in ambient photoperiod (Fig. 2). Beginning with an average body weight of 32.3 ± 3.4 g in October, ND body weight decreased by 17.3% to a minimum of 26.7 ± 2.1 g in January, followed by a weight gain of 53.9% to a body weight of 41.1 ± 3.9 g in April Control group animals kept in constant LD photoperiod (16 : 8 h light : dark) maintained an average body weight of 38.3 ± 3.6 g throughout the 6 months of the experiment. As a result, mean body weights of ND and LD animals differed by 12 g in January ($P < 0.01$), and were also significantly different in November ($P < 0.05$).

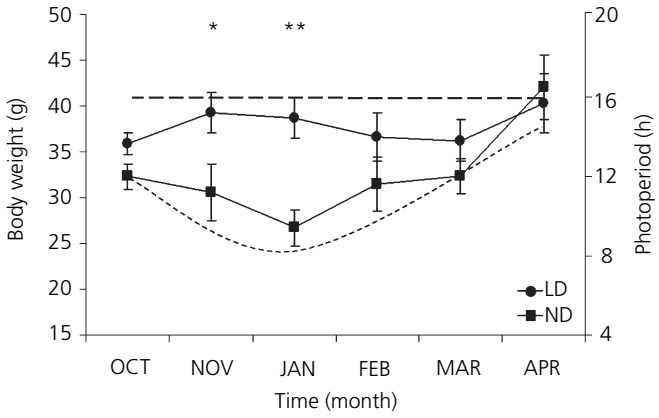

FIG. 2. Body weight of Siberian hamsters kept in constant long day (LD) (16 : 8 h light : dark; dashed line) or dynamic natural-day (ND) photoperiod (day length depending on ambient light during winter; dotted line) over 6 months from October until April (means ± SEM, n = 6 per time point). Photoperiod ranged from a minimum of 8.07 h light in January to a maximum of 14.19 h light in April. **P < 0.01; *P < 0.05, ND versus LD.

Effect of natural photoperiod on gene expression of PC1/3 and PC2

PC1/3 and PC2 mRNA were detected in various areas of the hamster hypothalamus with region-specific intensity differences (Fig. 3). Gene expression of both PC1/3 and PC2 was observed in ARC, paraventricular nucleus (PVN) and ventromedial nucleus (VMH), although gene expression in the PVN and VMH was close to the limit of detection and consequently was not quantified. In addition, PC1/3 mRNA was observed in the LH. Autoradiographs of PC1/3 and PC2 in the ARC revealed similar expression patterns to previously observed POMC mRNA distribution in this area (10). In addition, high concentrations of PC2 mRNA were observed in a small group of neurones within the dorsal medial posterior part of the arcuate nucleus (dmpARC).

Gene expression of PC1/3 within the ARC (Fig. 4A) and LH (Fig. 4B) revealed a significant overall effect of photoperiod ($P < 0.05$ for both regions) with higher levels of mRNA in ND (versus LD controls). However, PC1/3 mRNA levels in the ARC and LH were not correlated with the profile of changing photoperiod in ND; there were no effects of time (month) and no time × photoperiod interaction. In the LH (Fig. 4B), the apparent reflection of ND photoperiod in trends to increased levels of PC1/3 mRNA from October until January followed by a decline to February were not statistically significant.

Gene expression of PC2 in the ARC (Fig. 4C) and the dmpARC (Fig. 4D) also revealed strong effects of photoperiod with higher levels of mRNA in ND ($P < 0.001$ for both

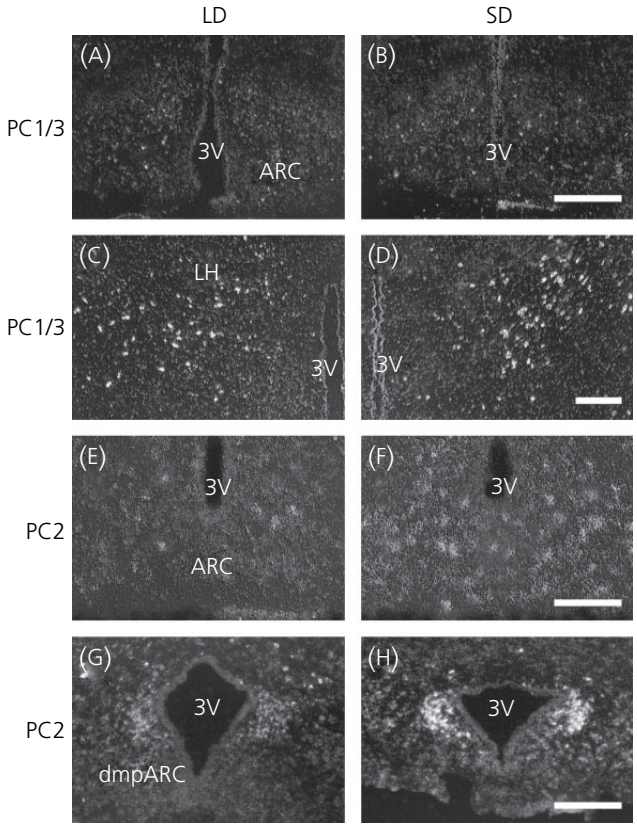

FIG. 3. Representative dark-field micrographs of autoradiographs showing gene expression of prohormone convertases 1/3 (PC1/3) and 2 (PC2) in quantified areas of the hypothalamus in long day (LD) and short day (SD) animals. Scale bars = 80 μm (A–B, E–H) and 100 μm (C–D).

regions). In addition, a seasonal pattern of PC2 gene expression in the ARC (Fig. 4C, quantified area excluding the dmpARC) was observed in ND hamsters (two-way ANOVA: $P < 0.01$ for effect of time; $P < 0.05$ for time × photoperiod interaction) with maximal mRNA levels observed in January (multiple comparison: $P < 0.05$). Although a similar temporal gene expression profile was apparent for gene expression of PC2 in the dmpARC (and for PC1/3 in LH), this could not be consolidated statistically (Fig. 4D).

Effect of transfer of hamsters from SD to LD on body weight

Body weights of the Siberian hamsters used in these experiments have been documented previously (29). Fourteen weeks in SD resulted in a 27% reduction in body weight, compared to LD controls. Transfer back to LD had little effect on body weight for the first 2 weeks but, thereafter, body weight increased significantly ($P < 0.001$) and achieved a level similar to that of LD controls by 6 weeks.

Effect of transfer of hamsters from SD to LD on gene expression of PC1/3 and PC2

Gene expression of PC1/3 in the ARC and LH did not change significantly after 14 weeks in SD (Fig. 4E,F, week 0). PC1/3 mRNA levels in the ARC and LH were unaffected by transfer from SD back to LD photoperiod (week 2, week 4, week 6) and were similar to those of LD controls. There were no effects of photoperiod or time, and no interaction. Neuroanatomical distribution patterns of PC1/3 mRNA analysed by emulsion autoradiography in the ARC (Fig. 3A–B) and LH (Fig. 3C–D) of SD and LD (week 0) also showed no apparent differences.

Photoperiod had no overall effect on PC2 gene expression in the ARC (Fig. 4G) or dmpARC (Fig. 4H) but PC2 gene expression revealed a significant effect of time ($P < 0.001$ for both regions), and a time × photoperiod interaction ($P < 0.001$ for both regions). Significantly higher levels of PC2 mRNA were found in the ARC ($P < 0.05$) and dmpARC ($P < 0.05$) of SD animals compared to LD controls after 14 weeks in SD photoperiod (week 0). This observation was corroborated by emulsion autoradiographs showing a higher content of silver grains with PC2 probes within the ARC (Fig. 3E–F) and dmpARC (Fig. 3G–H) of SD hamsters at time point week 0. Following the transfer from SD back to LD photoperiod, gene expression of PC2 in the ARC decreased to a nadir at week 4. A significant down regulation of gene expression was observed after transfer from SD back to LD at all three time points (week 2, week 4, week 6; $P < 0.05$, versus week 0 SD, respectively). Between 4 and 6 weeks after transfer back to LD, mRNA levels of PC2 increased significantly ($P < 0.05$). In the dmpARC, gene expression of PC2 was decreased after 2 weeks and remained significantly lower until 6 weeks (week 2, week 4, week 6; $P < 0.05$, versus week 0 SD, respectively) after transfer back to LD.

Effect of photoperiod on protein expression of PC1/3, PC2, POMC, ACTH, α-MSH, β-endorphin and orexin-A

Immunoreactive cells and fibres for PC1/3, PC2, POMC, ACTH, α-MSH, β-endorphin and orexin-A were observed in different hypothalamic areas of the Siberian hamster brain. Immunolocalised distribution patterns of PC1/3 and PC2 protein matched the mRNA pattern, except for a lack of PC2-ir in the dmpARC. Unlike the strong signal detected for PC2 mRNA in this region, little immunoreactivity for its protein could be observed (data not shown).

In the ARC, there was no effect of photoperiod on the number of counted PC1/3-ir cells (Fig. 5A,B, a-b); hamsters kept in LD had 167 ± 15 ir-cells and those in SD 153 ± 11 ir-cells within the investigated region of the ARC. However immunohistochemical staining of PC2 in the ARC showed 125% more ir-cells in SD (88 ± 19 ir-cells), leading to a significant difference ($P < 0.01$) compared to those counted in LD controls (39 ± 6 ir-cells) (Fig. 5A,B, c-d). POMC-ir in LD (178 ± 22 ir-cells) and SD (156 ± 10 ir-cells) revealed no significant difference in ir-cell number (Fig. 5A,B, e-f). ACTH-ir (LD, 105 ± 14; SD, 81 ± 9 ir-cells) as well as α-MSH-ir (LD, 47 ± 11; SD, 54 ± 13 ir-cells) levels in the ARC were also unaffected by photoperiod (Fig. 5A,B, g–h,k–l). By contrast, the density of α-MSH-ir fibres appeared greater in SD, but was not quantifiable (Fig. 5A,B, k–l). The neuroanatomical distribution pattern of β-endorphin-ir was similar to that of α-MSH-ir, but was mainly concentrated in cell bodies. Counting of β-endorphin-ir cells revealed 76%

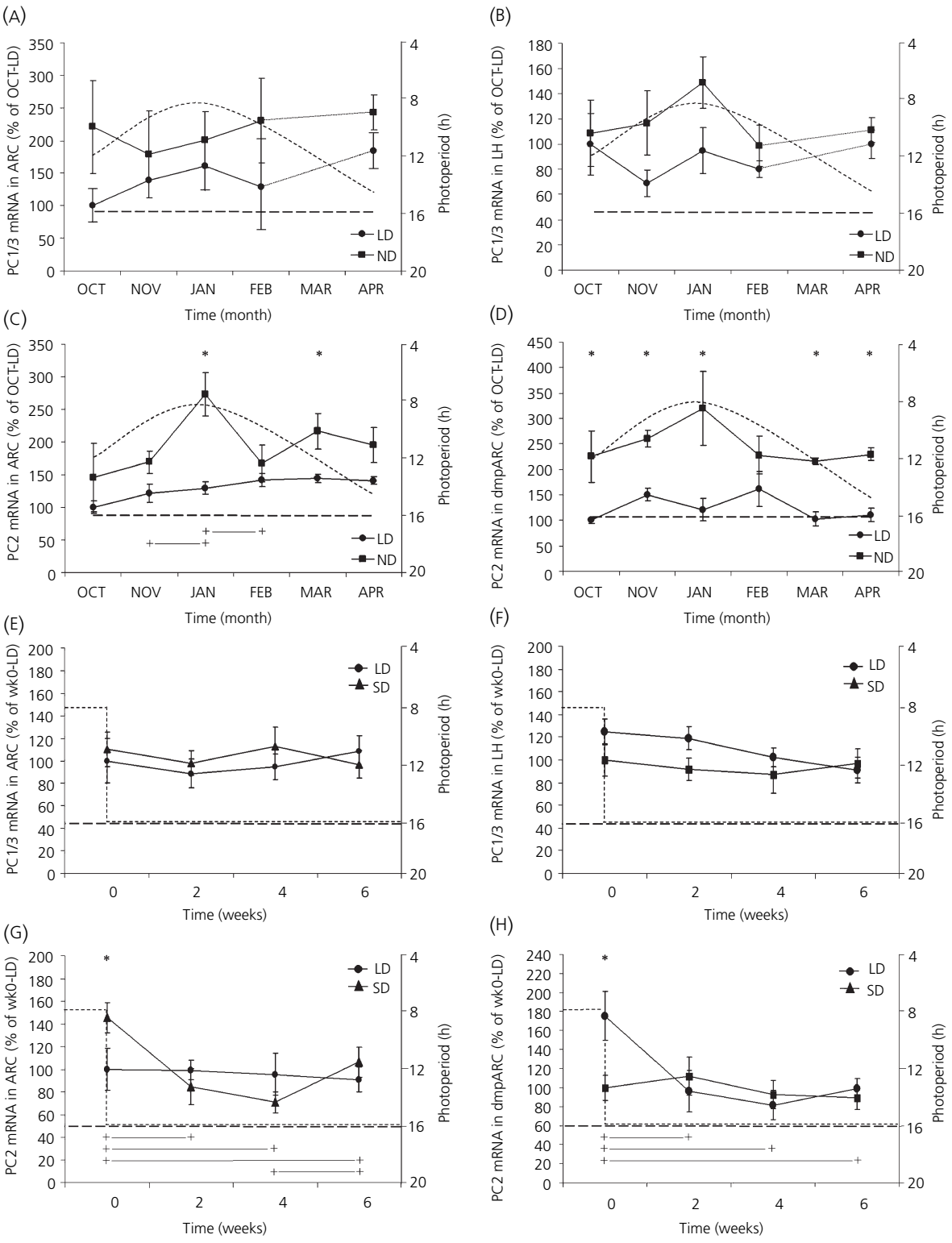

FIG. 4. Gene expression of prohormone convertases 1/3 (PC1/3) and 2 (PC2) in selected areas of the Siberian hamster hypothalamus. (A–D) Effect of changing photoperiod during winter on expression of PC1/3 (A, ARC; B, LH) and PC2 (C, ARC; D, dmpARC) genes. mRNA levels are expressed as mean percentages of LD controls in October (± SEM, n = 6 per time point). (E–H) PC1/3 (E, ARC; F, LH) and PC2 (G, ARC; H, dmpARC) gene expression after switch from SD (week 0) back to LD (week 2, week 4, week 6) photoperiod. mRNA levels are expressed as mean percentages of LD controls at week 0 (± SEM, n = 4 per group). LD is indicated by dashed lines, whereas dotted curves mark ND (A–D) or SD (E–H). Significances ($P < 0.05$) are marked by asterisks (*) for same time points but different photoperiods and crosses (+) for the same photoperiod (ND or SD, respectively) but at different time points.

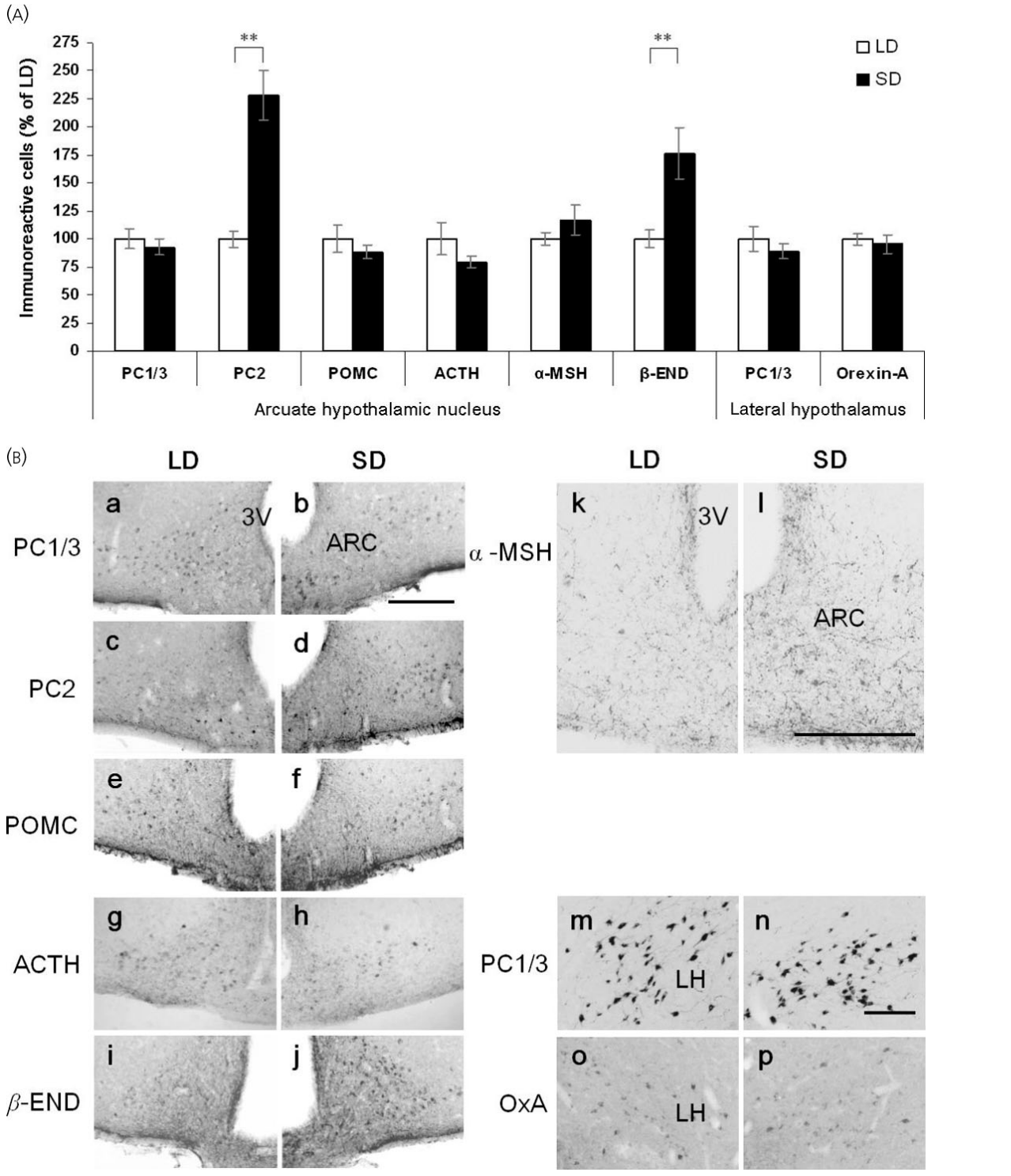

FIG. 5. (A) Quantitative analysis of immunoreactive (-ir) cells in selected areas of the Siberian hamster hypothalamus. Data are number of ir-cells expressed as percentage of long day (LD) controls (**$P < 0.01$, $n = 3$ per group). (B) Representative photomicrographs showing neuroanatomical distribution of immunoreactive cells in comparable hypothalamic areas of LD and short day (SD) animals. Colour inverted images of immunofluorescence stained sections (a–f, i–p) or peroxidase/substrate stained sections (g–h). 3V, Third ventricle; ARC, arcuate nucleus; LH, lateral hypothalamus. Scale bars = 100 μm (a–l) and 180 μm (m–p).

($P < 0.01$) more neurones in SD (74 ± 18 ir-cells) compared to LD (42 ± 9 ir-cells) (Fig. 5A,B, i–j). Quantification of PC1/3-ir (LD, 119 ± 16; SD, 104 ± 13 ir-cells) and orexin-A-ir (LD, 105 ± 14; SD, 97 ± 11 ir-cells) within the LH did not reveal differences between SD and LD controls (Fig. 5A,B, m–p).

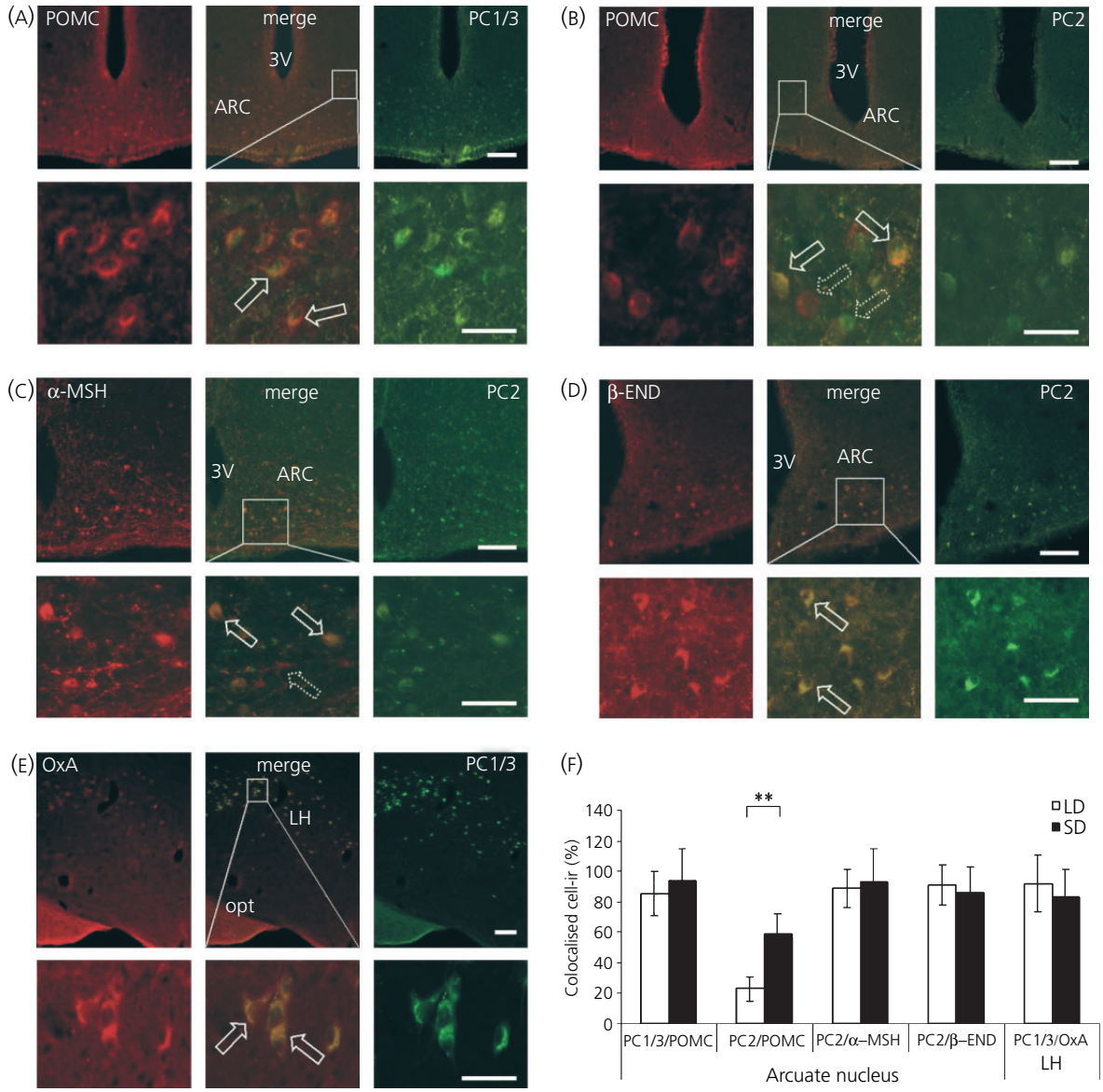

FIG. 6. (A–D) Photomicrographs showing immunofluorescence double staining of prohormone convertase 1/3 (PC1/3)-immunoreactivity (-ir) or prohormone convertase 2 (PC2)-ir with pro-opiomelanocortin (POMC)-ir and its derived neuropeptides in the arcuate nucleus and (E) PC1/3-ir and orexin-A-ir double staining in the lateral hypothalamus. Images derive from SD hamsters. For each panel, the upper row shows low magnification images and the lower row high magnification images of selected (boxed) areas. Merged images (centre) demonstrate colocalisation of immunoreactive products. Colocalisation is indicated by solid arrows, single cell-ir by dashed arrows. (F) Quantitative colocalisation analysis of prohormone convertase-ir (PC1/3 or PC2) and neuropeptide-ir. Values are expressed as mean percentages (± SEM) of counted POMC-ir, α-MSH-ir, β-endorphin-ir and orexin-A-ir cells in long day (LD) and short day (SD) (n = 3 per group). 3V, Third ventricle; ARC, arcuate nucleus; LH, lateral hypothalamus; opt, optical tract. Scale bars, low magnification images = 100 μm; high magnification images = 40 μm.

Effect of photoperiod on colocalisation of PC1/3 and PC2 with POMC, α-MSH, β-endorphin and orexin-A immunoreactivity

Dual fluorescence immunohistochemistry in the ARC showed no significant differences between the proportion of POMC-ir cells colocalised with PC1/3-ir cells in SD and LD. In both LD (87.5 ± 21%) and SD (94.1 ± 14.7%), nearly all POMC-ir cells were also PC1/3-ir positive (Fig. 6A,F). By contrast, the overall level of PC2-ir colocalisation with POMC-ir was lower and revealed significantly ($P < 0.01$) more POMC-ir cells which also contained PC2-ir in SD (59.14 ± 12.9%) than in LD (22.9 ± 8%) (Fig. 6B,F). Colocalisation of PC2-ir cells with α-MSH and β-endorphin immunoreactivity (Fig. 6C,D) revealed a nearly complete match of these POMC derived neuropeptides and the cleavage mediating prohormone convertase in SD and LD (Fig. 6F; α-MSH, LD, 89.1 ± 12.6%; SD, 93.2 ± 21.5%; β-endorphin, LD, 90.9 ± 13.5%; SD, 86.4 ± 16.3%). In the LH, there was no effect of photoperiod on the colocalisation of orexin-A-ir and PC1/3-ir (Fig. 6E,F); the neuropeptide product of prepro-orexin was localised with the majority of PC1/3-ir cells in this area in both LD (92 ± 18.4%) and SD (83.2 ± 18.7%).

Discussion

Seasonal body weight in mammals is regulated by a complex interaction of neuropeptides in a hypothalamic network of neurones that integrates environmental photoperiod inputs. Most of these energy balance-regulating neuropeptides are derived from larger biologically inactive precursors and have to undergo post-translational processing by endoproteolytic cleavage. The present study presents evidence substantiating the hypothesis that an important part of the photoperiod-driven regulation of POMC product biosynthesis is mediated by post-translational processing through PC1/3 and PC2, and thus provides valuable information over and above the control of precursor gene expression at a transcriptional level.

Neuroanatomical distribution patterns of PC1/3 and PC2 transcripts in the hamster hypothalamus match with previously described localisations in other rodent species such as rats and mice (21, 30). Hamsters kept in ND and SD displayed typical physiological adaptations to shortening or short photoperiod, including change of coat colour, reduction of reproductive tissue, reduced food intake and body weight loss. These photoperiod-induced physiological changes were not accompanied by temporal change in PC1/3 mRNA levels. Gene expression of PC1/3 in ARC and LH was higher overall in ND (versus LD) but this effect was not observed after 14 weeks in SD (versus LD) artificial photoperiod, suggesting some impact of prior photoperiodic history. At present, there is no clear explanation for this unexpected difference between ND and SD because gene expression of PC1/3 in summer ND (May to September) was not measured. Furthermore, short-term change of photoperiod induced by transfer from SD to LD was also without discernible effect on gene expression of PC1/3 in ARC and LH, suggesting that, on a transcriptional level, PC1/3 is not directly regulated by photoperiodic inputs. However, previous observations have demonstrated a regulatory effect of the adipose tissue hormone, leptin, on gene expression of PC1/3 in LH and ARC because reduced PC1/3 mRNA levels observed in obese *ob*/*ob* mice were up-regulated in response to leptin injection (31). Although PC1/3 gene expression appears to be sensitive to leptin in this natural knockout model, contrary to expectation, in Siberian hamsters, PC1/3 gene expression appears to be independent of seasonal modulation of leptin, despite the effect of photoperiod on this hormone (32). This suggests that the adipose tissue signal may be responsible for the maintenance of basal PC1/3 gene expression level.

By contrast to PC1/3, gene expression of PC2 in the ARC and dmpARC broadly paralleled the profile of changing ambient ND photoperiod in winter resulting in elevated mRNA when photoperiod was shortest. This photoperiod dependency was substantiated by up-regulated PC2 gene expression in hamsters kept in SD for 14 weeks. After transfer from SD to LD, mRNA levels of PC2 decreased rapidly and, within 2 weeks, levels were similar to those in LD. This acute regulatory change in PC2 gene expression preceded body weight loss and is therefore unlikely to be a secondary effect of metabolic and physiological changes. The photoperiod-driven gene expression profile suggests that PC2 may be an important part of a molecular neuroendocrine mechanism that is closely related to the integration of photoperiod information and the mediation of seasonal responses. Previous studies demonstrated a photoperiod-dependent differential gene expression of the neuropeptide precursor POMC in the ARC with lower mRNA levels in SD (11, 33). Initially, this observation appears paradoxical because down-regulation of POMC would most likely result in lower levels of its derived neuropeptide, α-MSH, whereas photoperiod-induced changes in metabolism and physiology such as reduced food intake and body weight loss would appear to require a higher concentration of the anorexic peptide, α-MSH. Artificial square-wave photoperiod transformation did not affect gene expression of PC1/3 and, consequently, cleavage activity of PC1/3 most likely results in unaltered levels of larger POMC derivates such as ACTH and β-lipotrophin, which are generated by PC1/3 cleavage. By contrast, increased gene expression of PC2 in SD is likely to increase proteolytic activity of PC2 at specific cleavage sites resulting in higher levels of smaller peptides such as α-MSH, β-MSH, γ-MSH, β-endorphin and corticotrophin- like intermediate peptide.

Despite reported decreased gene expression of POMC in SD, protein distribution in neurones of the ARC remained unaltered by photoperiod, suggesting that gene expression may not be the primary regulator of POMC product biosynthesis. Gene expression of PC1/3 in SD (versus LD) animals was also unaffected by photoperiod and was reflected in similar levels of PC1/3 protein in SD and LD acclimated hamsters. The regulation of PC2 transcript by photoperiod in the ARC was also reflected at a translational level because there was more PC2 protein detected in SD than LD animals. Similar levels of PC1/3 and POMC protein in SD and LD are reflected in unaltered ACTH-ir, with ACTH peptide known to be a direct result of POMC cleavage by PC1/3 (34). Although inhibitory properties of ACTH on food intake (35) would presume an accumulation of this peptide in SD animals, our results imply a minor role in regulation of seasonal body weight. By contrast, increased PC2 protein in SD animals was accompanied by higher levels of α-MSH-ir fibres and β-endorphin-ir cells, in line with previous studies demonstrating that α-MSH production varies directly in accordance with the expression of PC2 (36). Similar observations were reported for the maturation of β-endorphin (37). Interestingly, the fate of β-endorphin after its cleavage from β-lipotrophin is more extensive than that of α-MSH, and the implications of the observed immunoreactive protein levels are worthy of further consideration. The initially generated β-endorphin$_{1-31}$ is further processed to β-endorphin$_{1-27}$ and β-endorphin$_{1-26}$ (Fig. 1), which are considered to be opiate receptor antagonists opposing the effects of β-endorphin$_{1-31}$ (38). Whereas proteolytic processing of β-endorphin$_{1-27}$ is solely mediated by PC2 activity (39) and removal of the terminal basic residue of β-endorphin$_{1-27}$ by carboxypeptidase's E yields β-endorphin$_{1-26}$ (40), the cleavage of β-lipotrophin to β-endorphin$_{1-31}$ by PC2 is contentious. *In vivo* studies scrutinising β-endorphin$_{1-31}$ levels by radioimmunoassay in PC2-deficient mouse hypothalamus reported increased β-endorphin$_{1-31}$ levels despite PC2 inactivity, suggesting that β-endorphin$_{1-31}$ is likely to be a PC2 substrate rather than a direct product (18). In contrast, *in vitro* studies performed on AtT-20 anterior pituitary cells overexpressing

PC2 demonstrated enhanced conversion of β-lipotrophin to β-endorphin$_{1-31}$ (41). Another experiment performed *in vivo* in the hypothalamus of mice lacking functional PC2 found the processing of β-lipotrophin to β-endorphin$_{1-31}$ diminished by two-thirds. This result suggests that a minor part of the proteolytic conversion from β-lipotrophin to β-endorphin$_{1-31}$ could be mediated by a supplementary processing of the β-lipotrophin substrate by PC1/3 (42). The polyclonal antibody against β-endorphin used in the present study reacts with epitopes of all three β-endorphin forms (1-31, 1-27, 1-26) and hence displays immunoreactivity of total β-endorphin. However, in the hypothalamus, β-endorphin$_{1-31}$ constitutes more than 60% of the total β-endorphin-ir, in contrast to less than 30% β-endorphin$_{1\text{-}27\ +\ 1\text{-}26}$-like immunoreactivity (43). Our results corroborate these findings because PC2 up-regulation in SD results in higher concentrations of total β-endorphin. Current opinions on the physiological function of β-endorphin are conflicting; pharmacological studies generally indicate a short-term stimulatory effect of opioids on food intake (44, 45), but longer term regulation of energy balance has not been reported (46, 47), although β-END$^{-/-}$ mice (48) are characterised by an obese phenotype. This latter finding may support our observation of increased β-endorphin protein levels in states of reduced feeding behaviour and negative energy balance in SD, and the time scale over which these changes are manifested. These characteristics are consistent with our results because seasonal regulation of energy balance is a long-term process rather than an acute induced inhibition of food intake. An opposing and antagonistic effect of the processed β-endorphin$_{1-27}$, evidently a cleavage product mediated exclusively by PC2 activity (39), on opioid receptors could be an interesting target for further experiments attempting to explain this observation. By contrast to immunoreactivity of β-endorphin, which is more confined to the cell body, α-MSH-ir was widely distributed throughout fibres and boutons of neurones in the ARC. Thus, the biological relevance of quantification of relative α-MSH protein content by counting of ir-neurones is questionable. Appraisal of SD and LD α-MSH-ir distribution patterns revealed more intense staining of α-MSH-ir fibres in SD and hence higher levels of protein in SD. This observation is supported by the fact that the concentrations of α-MSH and β-endorphin are closely correlated, in agreement with their production in equimolar amounts as products of the same precursor (49).

Therefore, it is unlikely that less α-MSH than β-endorphin is processed and the immunoreactivity patterns observed in the present study could reflect different rates of transport and routes of intracellular trafficking within the neuronal network. Visually apparent increased levels of α-MSH could be appropriate to the state of negative energy balance in SD (7, 50). Combined with increased expression of β-endorphin in SD, these findings suggest a complementary interaction between the melanocortin, α-MSH, and the opioid, β-endorphin, on seasonal regulation of energy homeostasis, rather than opposing effects.

Colocalisation of PC1/3-ir with POMC-ir in ARC showed almost complete coexpression. This observation implies that cleavage of POMC by PC1/3 is a fundamental process that provides the same relative amounts of PC1/3-cleaved POMC-derived peptides independent of changing photoperiod in SD. We substantiated this hypothesis by demonstrating levels of ACTH-ir that were nearly equal in SD and LD. Even though we did not scrutinise the proteolytic processing fate of β-lipotrophin, the intermediate precursor of β-endorphin, similar results would be expected because β-lipotrophin is cleaved by PC1/3 in a similar manner to ACTH. α-MSH and β-endorphin were almost completely colocalised with PC2 in SD and LD reflecting their derivation from larger intermediate POMC fragments by proteolytic PC2 processing. As a result of higher protein concentrations of PC2 in SD (versus LD), more α-MSH-ir and β-endorphin-ir was processed and could be observed in animals that were exposed to short photoperiod.

The precise involvement of the hypocretins, orexins A and B, in feeding behaviour remains uncertain. Whereas early studies demonstrated an orexigenic effect (51), more recent observations suggest a more complex influence of both neuropeptides on energy balance. In particular, the role of orexin-B remains controversial with only a weak effect on food intake (52). By contrast, the orexin-A-induced hyperphagia and effects (increase) on metabolic rate are more robust (53). However, the exact mechanism by which orexin-A exerts its orexigenic action is not fully elucidated. Orexin-A and orexin-B are highly specifically localised in the LH and are generated by proteolytic processing of the precursor peptide prepro-orexin (54), whose gene expression in the LH was previously colocalised with mRNA encoding for PC1/3 (31). To date, the exact post-translational enzymatic mechanism by which prepro-orexin cleavage is mediated is unknown and there is no evidence from studies performed *in vivo* of direct PC1/3 involvement. Immunohistochemical colocalisation of PC1/3-ir and orexin-A-ir in the present study suggests a close relationship between these two neuroendocrine components at a protein level. Interestingly, virtually all orexin-positive neurones in the LH also express dynorphin (55), whose precursor molecule pro-dynorphin has been reported to be processed by PC1/3 in studies performed *in vitro* (56). Hence pro-dynorphin could be another possible target of PC1/3 activity within the orexin-ir positive neurones of the LH. Current evidence indicates that gene expression of prepro-orexin, such as that of PC1/3 in LH, is unaffected by photoperiod (10, 11). Our observations of equivalent levels of PC1/3-ir and orexin-A-ir are consistent with these published studies in SD and LD. In addition, we recently demonstrated that photoperiod had no effect on the second prepro-orexin derived neuropeptide, orexin-B, because no differences of orexin-B-ir were found in LH of SD and LD acclimated hamsters (57). Combined, these observations suggest that PC1/3 does not play a major role in the seasonal regulation of post translational neuropeptide maturation processes in the LH and hence in seasonal energy balance.

Interestingly, despite distinct gene expression of PC2 in dmpARC, immunoreactive protein was not observed and consequently the function of PC2 mRNA within these neurones remains unclear. This phenomenon could reflect rapid protein denaturation in this nucleus or the ability of neuronal cells to transport mRNA and perform protein biosynthesis in remote locations away from cell bodies (58, 59). Thus, PC2 mRNA could be transported to, and protein

synthesis located in, regions and areas within the hypothalamus other than its origin in the dmpARC. Post-translational modification of proPC2 to PC2 represents another possible explanation for the failure to detect PC2-ir (60). However, because of the polyclonal structure of the PC antibodies, a cross reaction with epitope sequences of the pro-forms should be possible. Neuronal projections from the dmpARC to other nuclei and the integration of dmpARC neurones in the hypothalamic neuroendocrine network remain to be established. There is growing evidence that the dmpARC is a functionally important component of the neuroendocrine network that regulates energy balance during seasonal adaptation; previous studies have identified a number of photoperiod regulated genes in this area (29, 61, 62). One of the identified neuropeptides within this subdivision of the ARC is the precursor proVGF, which is cleaved by PC1/3 and PC2 into biological active energy balance regulating peptides (63, 64). By contrast to VGF, where gene expression is increased in the dmpARC in SD but decreased in the ARC, gene expression of PC2 was up-regulated in both hypothalamic areas in SD. Interestingly, VGF-ir in the ARC is, like PC2-ir, also characterised by the apparent absence of protein in the dmpARC despite abundant mRNA expressed in this subnucleus (P. Barrett, unpublished data). Therefore PC2 might be transported away from its site of synthesis in the dmpARC very quickly to perform subsequent post-translational processing of proVGF at a different location of the CNS. ProVGF mRNA in the dmpARC suggests a possible target of post-translational PC2 activity as mRNA levels of proVGF are also significantly increased in SD hamsters and respond promptly, like gene expression of PC2, following photoperiod manipulation.

Thus, our results demonstrate that decreasing photoperiod up-regulates PC2 gene expression and PC2 protein, whereas gene expression and protein of PC1/3 are unaffected by SD. We hypothesise that this intensifies proteolytic processing of POMC intermediate derivatives (ACTH and β-lipotrophin), and is the reason for higher concentrations of POMC-derived α-MSH and β-endorphin in short photoperiod despite apparently paradoxical findings showing down-regulated POMC gene expression in SD. By contrast, unaltered PC1/3 gene expression and protein in LH and ARC suggests that regulation by photoperiod is not accomplished via proteolytic processing at PC1/3 specific sites. Thus, regulation of proteolytic processing activity by photoperiod via coordinated expression of PC1/3 and PC2 at transcriptional and translational levels is critical for the maturation of neuropeptide precursors.

Interestingly, the proteolytic enzymes, PC1/3 and PC2 not only mediate post-translational modifications, but are also targets of post-translational modification. First, both enzymes are initially synthesised as inactive precursor molecules, and propeptide cleavage is therefore necessary to activate the enzymes. Second, interaction with small associated neuroendocrine proteins such as proSAAS with PC1/3 (65) and dimerisation of 7B2 with PC2 (66) leads to an inhibition of their enzymatic activities, making these proteins important factors in the intracellular endocrine pathway. In particular, the dependency of PC2 activity on the presence of 7B2 is highly complex because the neuroendocrine protein 7B2 has also been implicated in the activation of the zymogene proPC2 *in vivo* (67). This initially paradoxical observation reflects the complex dimension of interactions between small associated neuroendocrine proteins and the regulation of proteolytic capacity of prohormone convertases. Because the influence of these proteins on the proteolytic activity is evidently most distinct, future studies should focus on these factors to elucidate the exact mechanisms by which photoperiodic regulation of propeptide synthesis is mediated.

The photoperiod-driven regulatory mechanism on a post-translational level observed in the present study could be an additional universal control point for other energy balance related neuropeptide precursors such as proNPY, proTRH and CART. In addition, we provide further evidence for the dmpARC as an area with distinct photoperiod influenced neuroendocrine activity, suggesting that this subdivision of hypothalamic arcuate neurones is an important integral part of the seasonal energy balance regulation network.

Acknowledgements

This collaborative study was funded by the Scottish Executive Environment and Rural Affairs Department (to J. G. Mercer) and EC FP6 funding ('DIABESITY' contract no. LSHM-CT-2003-503041 to J. G. Mercer), Deutsche Forschungsgemeinschaft (German Research Foundation KL973/5; to M. Klingenspor), the National Genome Research Network (NGFN 01GS0483; to M. Klingenspor) and the Danish Research Agency (to R. M. H. Khorooshi). M. Helwig was recipient of a fellowship funded by the European Commission to attend the ObeS[c]hool European Union Marie Curie Training Site at the Rowett Research Institute.

Accepted 3 March 2006

References

1 Mercer JG. Regulation of appetite and body weight in seasonal mammals. *Comp Biochem Physiol* 1998; **119:** 295–303.
2 Morgan PJ, Ross AW, Mercer JG, Barrett P. Photoperiodic programming of body weight through the neuroendocrine hypothalamus. *J Endocrinol* 2003; **177:** 27–34.
3 Schwartz MW, Woods SC, Porte D Jr, Seeley RJ, Baskin DG. Central nervous system control of food intake. *Nature* 2000; **404:** 661–671.
4 Mercer JG, Tups A. Neuropeptides and anticipatory changes in behaviour and physiology: seasonal body weight regulation in the Siberian hamster. *Eur J Pharmacol* 2003; **480:** 43–50.
5 Klingenspor M, Dickopp A, Heldmaier G, Klaus S. Short photoperiod reduces leptin gene expression in white and brown adipose tissue of Djungarian hamsters. *FEBS Lett* 1996; **399:** 290–294.
6 Tups A, Helwig M, Khorooshi RM, Archer ZA, Klingenspor M, Mercer JG. Circulating ghrelin levels and central ghrelin receptor expression are elevated in response to food deprivation in a seasonal mammal (*Phodopus sungorus*). *J Neuroendocrinol* 2004; **16:** 922–928.
7 Fan W, Boston B, Kesterson R, Hruby V, Cone R. Role of melanocortinergic neurons in feeding and the agouti obesity syndrome. *Nature* 1997; **385:** 165–168.
8 McMinn JE, Wilkinson CW, Havel PJ, Woods SC, Schwartz MW. Effect of intracerebroventricular alpha-MSH on food intake, adiposity, c-Fos induction, and neuropeptide expression. *Am J Physiol Regul Integr Comp Physiol* 2000; **279:** R695–R703.
9 Cone RD. The central melanocortin system and energy homeostasis. *Trends Endocrinol Metab* 1999; **10:** 211–216.
10 Mercer JG, Moar KM, Ross AW, Hoggard N, Morgan PJ. Photoperiod regulates arcuate nucleus POMC, AGRP, and leptin receptor mRNA in the Siberian hamster hypothalamus. *Am J Physiol Regul Integr Comp Physiol* 2000; **278:** R271–R281.

11 Reddy AB, Cronin AS, Ford H, Ebling FJ. Seasonal regulation of food intake and body weight in the male Siberian hamster. Studies of hypothalamic orexin (hypocretin), neuropeptide Y (NPY) and pro-opiomelanocortin (POMC). *Eur J Neurosci* 1999; **11:** 3255–3264.

12 Atcha Z, Cagampang FR, Stirland JA, Morris ID, Brooks AN, Ebling FJ, Klingenspor M, Loudon AS. Leptin acts on metabolism in a photoperiod-dependent manner, but has no effect on reproductive function in the seasonally breeding Siberian hamster (*Phodopus sungorus*). *Endocrinology* 2000; **141:** 4128–4135.

13 Tanaka S. Comparative aspects of intracellular proteolytic processing of peptide hormone precursors: studies of proopiomelanocortin processing. *Zool Sci* 2003; **20:** 1183–1198.

14 Paquet L, Zhou A, Chang EY, Mains RE. Peptide biosynthetic processing. distinguishing prohormone convertases PC1 and PC2. *Mol Cell Endocrinol* 1996; **120:** 161–168.

15 Dey A, Xhu X, Carroll R, Turck CW, Stein J, Steiner DF. Biological processing of the cocaine and amphetamine-regulated transcript precursors by prohormone convertases, PC2 and PC1/3. *J Biol Chem* 2003; **278:** 15007–15014.

16 Miller R, Toneff T, Vishnuvardhan D, Beinfeld M, Hook VY. Selective roles for the PC2 processing enzyme in the regulation of peptide neurotransmitter levels in brain and peripheral neuroendocrine tissues of PC2 deficient mice. *Neuropeptides* 2003; **37:** 140–148.

17 Laurent V, Jaubert-Miazza L, Desjardins R, Day R, Lindberg I. Biosynthesis of proopiomelanocortin-derived peptides in prohormone convertase 2 and 7B2 null mice. *Endocrinology* 2004; **145:** 519–528.

18 Miller R, Aaron W, Toneff T, Vishnuvardhan D, Beinfeld MC, Hook VY. Obliteration of alpha-melanocyte-stimulating hormone derived from POMC in pituitary and brains of PC2-deficient mice. *J Neurochem* 2003; **86:** 556–563.

19 Benjannet S, Rondeau N, Day R, Chretien M, Seidah NG. PC1 and PC2 are proprotein convertases capable of cleaving proopiomelanocortin at distinct pairs of basic residues. *Proc Natl Acad Sci USA* 1991; **88:** 3564–3568.

20 Thomas L, Leduc R, Thorne BA, Smeekens SP, Steiner DF, Thomas G. Kex2-like endoproteases PC2 and PC3 accurately cleave a model prohormone in mammalian cells: evidence for a common core of neuroendocrine processing enzymes. *Proc Acad Sci USA* 1991; **88:** 5297–5301.

21 Schafer MKH, Day R, Cullinan WE, Chrétien M, Seidah NG, Watson SJ. Gene expression of prohormone an proprotein convertases in the rat CNS. A comparative in situ hybridisation analysis. *J Neurosci* 1993; **13:** 1258–1279.

22 Brobeck JR. Mechanism of the development of obesity in animals with hypothalamic lesions. *Physiol Rev* 1946; **26:** 541–559.

23 Watson SJ, Khachaturian H, Taylor L, Fischli W, Goldstein A, Akil H. Pro-dynorphin peptides are found in the same neurons throughout rat brain: immunocytochemical study. *Proc Natl Acad Sci USA* 1983; **80:** 891–894.

24 Zamir N, Skofitsch G, Bannon MJ, Jacobowitz DM. Melanin-concentrating hormone: unique peptide neuronal system in the rat brain and pituitary gland. *Proc Natl Acad Sci USA* 1986; **83:** 1528–1531.

25 de Lecea L, Kilduff TS, Peyron C, Gao X, Foye PE, Danielson PE, Fukuhara C, Battenberg EL, Gautvik VT, Bartlett FS, 2nd Frankel WN, van den Pol AN, Bloom FE, Gautvik KM, Sutcliffe JG. The hypocretins: hypothalamus-specific peptides with neuroexcitatory activity. *Proc Natl Acad Sci USA* 1998; **95:** 322–327.

26 Klingenspor M, Niggemann H, Heldmaier G. Modulation of leptin sensitivity by short photoperiod acclimation in the Djungarian hamster, *Phodopus sungorus*. *J Comp Physiol [B]* 2000; **170:** 37–43.

27 Morin LP, Wood RI. *A Sterotaxic Atlas of the Golden Hamster Brain*. San Diego, CA: Academic Press, 2001.

28 Simmens DM, Arriza JL, Swanson LW. A complete protocol for *in situ* hybridisation of messenger RNAs in brain and other tissues with radiolabeled single-stranded RNA probes. *J Histotechnol* 1989; **12:** 169–181.

29 Ross AW, Bell LM, Littlewood PA, Mercer JG, Barrett P, Morgan PJ. Temporal changes in gene expression in the arcuate nucleus precede seasonal responses in adiposity and reproduction. *Endocrinology* 2005; **146:** 1940–1947.

30 Seidah NG, Marcinkiewicz M, Benjannet S, Gaspar L, Beaubien G, Mattei MG, Lazure C, Mbikay M, Chretien M. Cloning and primary sequence of a mouse candidate prohormone convertase PC1 homologous to PC2, Furin, and Kex2: distinct chromosomal localization and messenger RNA distribution in brain and pituitary compared to. *Pc2, Mol Endocrinol* 1991; **5:** 111–122.

31 Nilaweera KN, Barrett P, Mercer JG, Morgan PJ. Precursor-protein convertase 1 gene expression in the mouse hypothalamus. differential regulation by ob gene mutation, energy deficit and administration of leptin, and co expression with prepro-orexin. *Neuroscience* 2003; **119:** 713–720.

32 Williams G, Cai XJ, Elliott JC, Harrold JA. Anabolic neuropeptides. *Physiol Behav* 2004; **81:** 211–222.

33 Mercer JG, Moar KM, Ross AW, Morgan PJ. Regulation of leptin receptor, POMC, and AGRP gene expression by photoperiod in the hypothalamic nucleus of the male Siberian hamster (*Phodopus sungorus*). *Appetite* 2000; **34:** 109–111.

34 Friedman TC, Loh YP, Birch NP. In vitro processing of proopiomelanocortin by recombinant PC1 (SPC3). *Endocrinology* 1994; **135:** 854–862.

35 Al-Barazanji KA, Miller JE, Rice SQ, Arch JR, Chambers JK. C-terminal fragments of ACTH stimulate feeding in fasted rats. *Horm Metab Res* 2001; **33:** 440–445.

36 Kato H, Kuwako K, Suzuki M, Tanaka S. Gene expression patterns of pro-opiomelanocortin-processing enzymes PC1 and PC2 during postnatal development of rat corticotrophs. *J Histochem Cytochem* 2004; **52:** 943–957.

37 Marcinikewicz M, Day R, Seidah NG, Chretien M. Ontogeny of the prohormone convertases PC1 and PC2 in the mouse hypophysis and their colocalization with corticotropin and alpha-melanotropin. *Proc Natl Acad Sci USA* 1993; **90:** 4922–4926.

38 Hammonds RG Jr, Nicolas P, Li CH. beta-endorphin-(1-27) is an antagonist of beta-endorphin analgesia. *Proc Natl Acad Sci USA* 1984; **81:** 1389–1390.

39 Zhou A, Bloomquist BT, Mains RE. The prohormone convertases PC1 and PC2 mediate distinct endoproteolytic cleavages in a strict temporal order during proopiomelanocortin biosynthetic processing. *J Biol Chem* 1993; **268:** 1763–1769.

40 Fricker LD. Carboxypeptidase E. *Annu Rev Physiol* 1988; **50:** 309–321.

41 Zhou A, Mains RE. Endoproteolytic processing of proopiomelanocortin and prohormone convertases 1 and 2 in neuroendocrine cells overexpressing prohormone convertases 1 or 2. *J Biol Chem* 1994; **269:** 17440–17447.

42 Allen RG, Peng B, Pellegrino MJ, Miller ED, Grandy DK, Lundblad JR, Washburn CL, Pintar JE. Altered processing of pro-orphanin FQ/nociceptin and pro-opiomelanocortin-derived peptides in the brains of mice expressing defective prohormone convertase 2. *J Neurosci* 2001; **21:** 5864–5870.

43 Millington WR, Smith DL. The posttranslational processing of beta-endorphin in human hypothalamus. *J Neurochem* 1991; **57:** 775–781.

44 Glass MJ, Billington CJ, Levine AS. Opioids and food intake: distributed functional neuronal pathways? *Neuropeptides* 1999; **33:** 360–368.

45 Kalra SP, Horvath TL. Neuroendocrine interactions between galanin, opioids, and neuropeptide Y in the control of reproduction and appetite. *Ann NY Acad Sci* 1998; **863:** 236–240.

46 de Zwaan M, Mitchell JE. Opiate antagonists and eating behaviour in humans: a review. *J Clin Pharmacol* 1992; **32:** 1060–1072.

47 Levine AS, Billington CJ. Opioids. Are they regulators of feeding? *Ann NY Acad Sci* 1989; **575:** 209–219.

48 Appleyard SM, Hayward M, Young JI, Butler AA, Cone RD, Rubinstein M, Low MJ. A role of endogenous opioids beta-endorphin in energy homeostasis. *Endocrinology* 2003; **144:** 1753–1760.

49 Bertagna X. Proopiomelanocortin-derived peptides. *Endocrinol Metab Clin North Am* 1994; **23:** 467–485.

50 Brown KS, Gentry RM, Rowland NE. Central injection in rats of alpha-melanocyte stimulating hormone analog: effects on food intake and brain Fos. *Regul Pept* 1998; **78:** 89–94.

51 Sakurai T, Amemiya A, Ishii M, Matsuzaki I, Chemelli RM, Tanaka H, Williams SC, Richarson JA, Kozlowski GP, Wilson S, Arch JR, Buckingham RE, Haynes AC, Carr SA, Annan RS, McNulty DE, Liu WS, Terrett JA, Elshourbagy NA, Bergsma DJ, Yanagisawa M. Orexins and orexin receptors: a family of hypothalamic neuropeptides and G protein-coupled receptors that regulate feeding behavior. *Cell* 1998; **92:** 696.

52 Edwards CM, Abusnana S, Sunter D, Murphy KG, Ghatei MA, Bloom SR. The effect of the orexins on food intake. comparison with neuropeptide Y, melanin-concentrating hormone and galanin. *J Endocrinol* 1999; **160:** R7–R12.
53 Haynes AC, Jackson B, Overend P, Buckingham RE, Wilson S, Tadayyon M, Arch JR. Effects of single and chronic intracerebroventricular administration of the orexins on feeding in the rat. *Peptides* 1999; **20:** 1099–1105.
54 Sakurai T, Moriguchi T, Furuya K, Kajiwara K, Nakamura T, Yanagisawa M, Goto K. Structure and function of human prepro-orexin gene. *J Biol Chem* 1999; **274:** 17771–17776.
55 Chou TC, Lee CE, Lu J, Elmquist JK, Hara J, Willie JT, Beuckmann CT, Chemelli RM, Sakurai T, Yanagisawa M, Saper CB, Scammell TE. Orexin (hypocretin) neurons contain dynorphin. *J Neurosci* 2001; **21:** RC168.
56 Dupuy A, Lindberg I, Zhou Y, Akil H, Lazure C, Chretien M, Seidah NG, Day R. Processing of prodynorphin by the prohormone convertase PC1 results in high molecular weight intermediate forms. Cleavage at a single arginine residue. *FEBS Lett* 1994; **337:** 60–65.
57 Khorooshi RM, Klingenspor M. Neuronal distribution of melanin-concentrating hormone, cocaine- and amphetamine-regulated transcript and orexin-B in the brain of the Djungarian hamster (*Phodopus sungorus*). *J Chem Neuroanatom* 2005; **29:** 137–148.
58 Lee SK, Hollenbeck PJ. Organization and translation of mRNA in sympathetic axons. *J Cell Sci* 2003; **116:** 4467–4478.
59 Koenig E, Giuditta A. Protein-synthesizing machinery in the axon compartment. *Neuroscience* 1999; **89:** 5–15.
60 Braks JA, Van Horssen AM, Martens GJ. Dissociation of the complex between the neuroendocrine chaperone 7B2 and prohormone convertase PC2 is not associated with proPC2 maturation. *Eur J Biochem* 1996; **238:** 505–510.
61 Barrett P, Ross AW, Balik A, Littlewood PA, Mercer JG, Moar KM, Sallmen T, Kaslin J, Panula P, Schuhler S, Ebling FJ, Ubeaud C, Morgan PJ. Photoperiodic regulation of histamine H3 receptor and VGF messenger ribonucleic acid in the arcuate nucleus of the Siberian hamster. *Endocrinology* 2005; **146:** 1930–1939.
62 Ross AW, Webster CA, Mercer JG, Moar KM, Ebling FJ, Schuhler S, Barrett P, Morgan PJ. Photoperiod regulation of hypothalamic retinoid signalling: association of retinoid X receptor gamma with body weight. *Endocrinology* 2004; **145:** 13–20.
63 Trani E, Giorgio A, Canu N, Amadoro G, Rinaldi AM, Halban PA, Ferri GL, Possenti R, Schinina ME, Levi A. Isolation and characterization of VGF peptides in rat brain. Role of PC1/3 and PC2 in the maturation of VGF precursor. *J Neurochem* 2002; **81:** 565–574.
64 Hahm S, Mizuno TM, Wu TJ, Wisor JP, Priest CA, Kozak CA, Boozer CN, Peng B, McEvoy RC, Good P, Kelley KA, Takahashi JS, Pintar JE, Roberts JL, Mobbs CV, Salton SR. Target deletion of the VGF gene indicates that the encoded secretory peptide precursor plays a novel role in the regulation of energy balance. *Neuron* 1999; **23:** 537–548.
65 Fricker LD, McKinzie AA, Sun J, Curran E, Qian Y, Yan L, Patterson SD, Courchesne PL, Richards B, Levin N, Mzhavia N, Devi LA, Douglass J. Identification and characterization of proSAAS, a granin-like neuroendocrine peptide precursor that inhibits prohormone processing. *J Neurosci* 2000; **20:** 639–648.
66 Mbikay M, Seidah NG, Chretien M. Neuroendocrine secretory protein 7B2: structure, expression and functions. *Biochem J* 2001; **357:** 329–342.
67 Westphal CH, Muller L, Zhou A, Zhu X, Bonner-Weir S, Schambelan M, Steiner DF, Lindberg I, Leder P. The neuroendocrine protein 7B2 is required for peptide hormone processing in vivo and provides a novel mechanism for pituitary Cushing's disease. *Cell* 1999; **96:** 689–700.

